Supporting Information

Malito et al. 10.1073/pnas.1201964109

SI Methods

Purification and Crystallization. Purified CRM197, showing a percentage of nicking of less than 5%, was frozen in the presence of phosphate-buffered saline at −20°C for 12 h. Dimeric CRM197 was subsequently isolated by size-exclusion chromatography in nonreducing conditions using as elution buffer 50 mM Tris [pH 8.0], 150 mM NaCl.

Crystallization experiments were performed in a nanodroplet sitting drop vapor diffusion format with 480 conditions screens performed at both 4 and 20 °C, using 96 well low profile Greiner plates. Crystals of nucleotide-free CRM197 were grown at 20 °C. Sitting drops were formed by mixing equal volumes (0.25 μL) of 20 mg/mL of CRM197 in crystallization buffer (50 mM Tris [pH 8.0], 150 mM NaCl), and of a well solution consisting of 1.9 M Ammonium Sulfate, 100 mM Bicine [pH 9.0]. Native CRM197 crystals belong to space group $C2$, with unit cell dimensions $a = 105.8, b = 91.3, c = 63.8$ and $\alpha = 90, \beta = 91.7, \gamma = 90$. The asymmetric unit contains one CRM197 molecule with a solvent content of 57% (Matthews coefficient 2.86 $Å^3$ Da^{-1}). Crystals of the complex nicotinamide-CRM197 were obtained by quickly soaking native (nucleotide-free) CRM197 crystals with a stabilizing solution made of 1.9 M Ammonium Sulfate, 100 mM Bicine [pH 9.0], plus 5 mM NAD^+. Crystals of the complexed form belong to space group $P1$, with unit cell dimensions $a = 65.6, b = 69.2, c = 69.6, \alpha = 98.3, \beta = 99.5, \gamma = 97.7$. The asymmetric unit contains two CRM197 monomers with a solvent content of 57% (Matthews coefficient 2.87 $Å^3$ Da^{-1}).

All crystals were mounted in cryoloops, using 10% Ethylene glycol as cryoprotectant prior to cooling to 100 K for data collection.

Data collection and structure determination. X-ray diffraction data were processed with HKL2000 (1) and iMosflm (2). The structures of nucleotide-free and nicotinamide complexed CRM197 were solved at 2.0 Å by molecular replacement in PHASER (3), using as search model coordinates of PDB ID code 1SGK. Refinement and model building were performed with PHENIX (4) and Coot (5).

The final refined model of nucleotide-free CRM197 includes residues 5–37, 50–187, 201–348, 354–516, and 520–535, and the final refined model of nicotinamide-CRM197 includes residues 1–37, 51–187, 200–349, 354–501, 504–516, and 520–535 for chain A, and 3–37, 51–187, 201–351, 354–516, and 521–535, for chain B.

All other crystallographic manipulations were carried out with the CCP4 package (6). Data collection and refinement statistics are shown in Table S1. Figures were generated with the program PYMOL (http://www.pymol.org).

Surface Plasmon Resonance (SPR), Biacore. For each titration, proteins were first covalently immobilized by amine-coupling on a carboxymethylated dextran sensor chip (CM-5, GE Healthcare). Amine-coupling reactions for immobilization of DT proteins were performed using purified protein at approximately 5 μg/mL in 10 mM sodium acetate buffer pH 5.5 injected at 5 μL/min until approximately 6,000 response units (RU) were captured. An unmodified surface was used as reference.

Titration experiments were performed by injecting at 30 μL/min NAD diluted in running buffer (filtered and degassed) containing Hepes Buffered Saline (HBS) with 0.05% Tween-20 pH 7.4, to final concentrations ranging from 0.75 μM to 200 μM. Following each 90-s injection, sensor chip surfaces were regenerated with a 20-s injection of 1 M NaCl. Each titration series contained 10 analyte injections including the blank. Data were analyzed using the BIAevaluation software; a blank injection of buffer only was subtracted from each curve and reference sensorgrams were subtracted from experimental sensorgrams to yield curves representing specific binding. The very fast association and dissociation rates yielded sensorgram curve shapes that did not enable fitting of sensorgrams to any BIAevaluation kinetic models. Therefore steady-state analysis was used to plot equilibrium binding response (R_{eq}) against analyte concentration in order to obtain the dissociation constants (K_D).

NAD-Glycohydrolase Activity Assay. The assay was carried out in 50 mM potassium phosphate, pH 7.5, 0.1 mM [*carbonyl*-^{14}C] NAD (0.05 μCi) in a total volume of 0.15 ml. The reactions were carried out in the presence or in the absence of 50 mM DTT. Samples (50 μL) after incubation at 37 °C for 18 h were applied to 1-mL column of Dowex AG 1-X2. The ^{14}C-nicotinamide produced by the catalyzed reaction was eluted with 5 mL of H_2O and the radioactivity quantified by liquid scintillation counting.

Molecular Dynamics Simulation. The proteins were solvated in TIP3P water box in the presence of 0.5 M NaCl. They were subjected to molecular dynamics simulation under periodic boundary conditions ($84 \times 110 \times 92$). Each simulation was initiated by minimizing the entire system in which protein backbone atoms were restrained with harmonic force of 10 kcal/molA2. Afterward the systems were heated from 0 K to 33 K and their volume equilibrated in four steps: The first step was 600 ps constant volume simulation in which protein backbone atoms were fixed; the second step was 600 ps constant volume simulation in which Ca protein atoms were restrained; the third step was 800 ps constant pressure (P = 1 bar) simulation with restrained C^{α} protein atoms; and the forth step was 1 ns simulation with the whole system relaxed. After the equilibration was completed, the systems were subjected to 8 ns constant pressure (P = 1 bar) and temperature (T = 330 K) MD run. The time step for integration was 2 fs, and the coordinates of all atoms were saved every 5 ps. Bonds involving hydrogen atoms were constrained via the SHAKE algorithm. A 12-Å cutoff distance was used for all nonbonded interactions. Long-range electrostatic forces were handled using the particle-mesh Ewald (7) algorithm. All simulations were performed using the NAMD software package (8) with charm27 force field.

All calculations were performed on Dell Precision T5500 workstation equipped with two 2.8 GHz Xeon X5660 six-core processors and two nVidia Quadro 5000 graphic cards. Each MD simulation was run in parallel distributed over 4 cores and utilizing graphic cards using NAMD code optimized for GPU computing.

It took on average 67 h to complete an 8-ns MD simulation run.

Thermofluor Assay/Differential Scanning Fluorimetry. A typical experiment was performed using a 96-well thin-wall PCR plate (Axigen). Monomeric forms of CRM197 and DT proteins were used at the final concentration of 2.5 μM. The SYPRO orange dye 5000X (Invitrogen), diluted 1:10 in 25 mM Tris-HCl, pH 7.5, was utilized at the final concentration of 5X in each well. The final volume of reaction mixtures were 40 μL in 25 mM Tris-HCl, pH 7.5. Fluorescence intensities were monitored in Stratagene Mx3005 RT-PCR instruments using the FAM

(492 nm) and ROX (610 nm) filters for excitation and emission, respectively. Samples were heated from 25 °C to 95 °C at scan rate of 1°C/ min. Tm values were extrapolated fitting the raw data to Boltzmann model (9) by GraphPad Prism 5.0 software.

1. Otwinowski Z, Minor W (1997) Processing of X-ray diffraction data collected in oscillation mode. *Methods Enzymol* 276:307–326.
2. Leslie AGW (2006) The integration of macromolecular diffraction data. *Acta Crystallogr D* 62:48–57.
3. McCoy A, et al. (2007) Phaser crystallographic software. *J Appl Crystallogr* 40:658–674.
4. Adams PD et al. (2010) PHENIX: A comprehensive Python-based system for macromolecular structure solution. *Acta Crystallogr D* 66:213–221.
5. Emsley P, Cowtan K (2004) Coot: Model-building tools for molecular graphics. *Acta Crystallogr D* 60:2126–2132.
6. Collaborative Computational Project Number 4 (1994) The CCP4 suite: Programs for protein crystallography. *Acta Crystallogr D* 50:760–763.
7. Darden T, York D, Pedersen L (1993) Particle mesh Ewald: An W log(N) method for Ewald sums in large systems. *J Chem Phys* 98:10089–10092.
8. Phillips JC, et al. (2005) Scalable molecular dynamics with NAMD. *J Comput Chem* 26:1781–1802.
9. Niesen FH, Berglund H, Vedadi M (2007) The use of differential scanning fluorimetry to detect ligand interactions that promote protein stability. *Nat Protoc* 2:2212–2221.

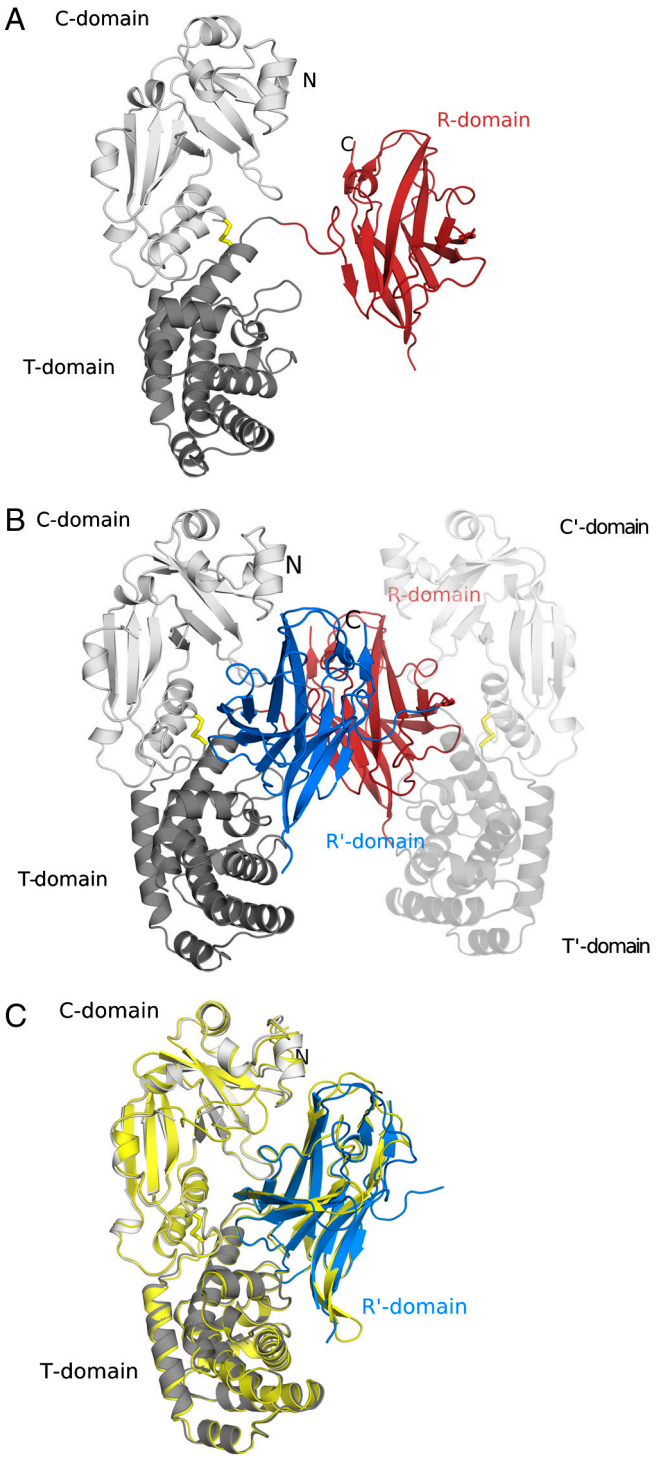

Fig. S1. Crystal structure of CRM197 and R domain swap. (*A*) The "open" monomer of nucleotide-free CRM197 is depicted as cartoon, and the catalytic (C) (residues 1–187), transmembrane (T) (residues 201–384), and receptor (R) (residues 387–535) domains are colored as light gray, dark gray, and red, respectively. The disulfide bond that covalently links fragment A (C domain) to fragment B (domains T and R) is shown as yellow sticks. (*B*) Dimeric CRM197 showing a twofold symmetry related molecule whose C, T, and R domains are labeled with primed letters. The domains are colored as in *A*, except for the R′ domain that is colored and labeled in blue. (*C*) "Closed" monomeric DT (PDB ID code 1MDT) is shown as yellow cartoon superimposed to CRM197 to show how the CT domains of CRM197 from one chain and the R′ domain from the second chain reconstitute the monomeric "closed" DT.

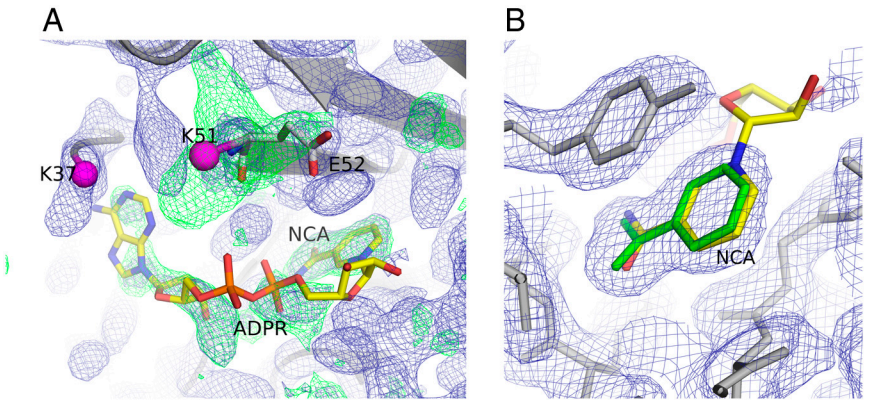

Fig. S2. (*A*) $1\sigma\ 2F_o - F_c$ (blue mesh) and $3\sigma\ F_o - F_c$ (green mesh) electron density maps of the dataset from the crystal of CRM197 soaked in 5 mM NAD after the first cycles of restrained refinement. The C domain is shown as a gray cartoon, and the last visible residues of the active-site loop are shown in magenta. NAD from PDB ID code 1TOX is superimposed onto CRM197 to show how the extra electron densities in the binding pocket of CRM197 partially explain the modeling of the ADP-ribose moiety while perfectly fit the nicotinamide moiety. Also, extra $F_o - F_c$ electron density is shown for E52 in place of G52. (*B*) Final $2F_o - F_c$ electron density map for NCA is shown as blue mesh. NCA bound to CRM is shown as green sticks, while superimposed NAD from NAD-DT is shown as sticks with carbon, nitrogen, and oxygen atoms colored in yellow, blue, and red, respectively. The protein residues of CRM197 are shown as gray sticks.

Table S1. Data collection and refinement statistics

	NF-CRM197	*NCA-CRM197*
Data collection		
Space group	*C*2	*P*1
Cell dimensions		
a, *b*, *c* (Å)	105.8, 91.3, 63.8	65.6, 69.2, 69.6
α, β, γ (°)	90, 91.7, 90	98.3, 99.5, 97.7
Resolution (Å)	2.0 (2.07)*	2.0 (2.1)*
R_{sym} or R_{merge}	8.1 (62.1)	5.1 (51)
$I/\sigma I$	24.2 (1.4)	8.8 (1.4)
Completeness (%)	97.8 (87.5)	90.3 (84.8)
Redundancy	3.6 (3.4)	1.9 (1.8)
Refinement		
Resolution (Å)	2.0	2.0
No. reflections	36,533	59,591
R_{work}/R_{free}	20.9/24.1	19.5/24.4
No. atoms		
Protein	3,662	7,477
Ligand/ion	-	36
Solvent	170	252
B-factors		
Protein	56.4	42
Ligand/ion	-	40.5
Water	53.4	35
R.m.s. deviations		
Bond lengths (Å)	0.007	0.007
Bond angles (°)	0.961	1.059

$R_{sym} = \sum_{hkl} \sum_i |I_i(hkl) - < I(hkl) > |/\sum_{hkl} \sum_i I_i(hkl)$.
$R_{work} = \sum ||F_{(obs)}| - |F_{(calc)}||/\sum |F_{(obs)}|$.
R_{free} = as for R_{work} but calculated for 5.0% of the total reflections that were chosen at random and omitted from refinement.
*Highest resolution shell is shown in parentheses.